Chemical Physics Letters 465 (2008) 20–24

Contents lists available at ScienceDirect

Chemical Physics Letters

journal homepage: www.elsevier.com/locate/cplett

# Photoionization of atmospheric gases studied by time-resolved terahertz spectroscopy

Zoltan Mics [a], Petr Kužel [a,*], Pavel Jungwirth [b], Stephen E. Bradforth [c]

[a] Institute of Physics, Academy of Sciences of the Czech Republic, Na Slovance 2, 182 21 Prague 8, Czech Republic
[b] Institute of Organic Chemistry and Biochemistry, Academy of Sciences of the Czech Republic, Center for Biomolecules and Complex Molecular Systems, Flemingovo nam. 2, 166 10 Prague 6, Czech Republic
[c] Department of Chemistry, University of Southern California, Los Angeles, CA 90089, USA

ARTICLE INFO

*Article history:*
Received 23 May 2008
In final form 17 September 2008
Available online 24 September 2008

ABSTRACT

We investigate the laser induced ionization and plasma formation in pure oxygen and nitrogen by means of optical pump–terahertz probe spectroscopy. Focused amplified femtosecond pulses at 405 and 810 nm are used to ionize the gas molecules by nonlinear processes. The ionized gas is probed by picosecond terahertz pulses in the frequency range of 0.2–2 THz to obtain the free electron density ($10^{13}$–$10^{17}$ $cm^{-3}$) and the electron scattering time (0.2 ps for $N_2$ and 0.4 ps for $O_2$). We demonstrate the importance of the centrifugal barrier for the photoionization process using circularly polarized light.



## 1. Introduction

Ionization of atoms or molecules at high laser fields has been subject of extensive research [1–3]. Femtosecond laser time-resolved studies of the gas plasma employ intense ultrashort laser pulses to ionize the examined gas [4–6]. In this regime the laser electric field amplitude in the range of $0.5–5 \times 10^8$ V/cm can be easily achieved (corresponding to tens or a few hundreds of TW/$cm^2$ peak pulse intensity). The forces these fields exert on the electrons are comparable to the binding forces of valence electrons in molecules leading to a number of interesting phenomena which cannot be simply described within the time-dependent perturbation theory.

Beside its contribution to laser plasmas generated in air [7], ionized gases (oxygen in particular) play an prominent role in the upper atmosphere. For example $O_2^+$ is an important atmospheric source of singlet oxygen atoms [8,9] which in turn are responsible for auroral radiation [10].

THz pulsed radiation has been shown to provide a powerful tool for probing the plasma in ionized gases [11–13]. Kampfrath et al. have been able to probe the dynamics of ionized $O_2$ and Ar gas by THz pulses in the frequency range 5–30 THz; from the evolution of the plasma properties the temperature of the free electron gas has been determined [14]. These successful applications of THz spectroscopy for plasma characterization are related to the fact that (i) the THz pulses are highly sensitive to the presence of mobile charge carriers and that (ii) optical pump–THz probe spectroscopy is able to provide time-resolved complex THz dielectric spectra. As a result it is possible to determine both the concentration and the momentum scattering rate of the charges in the plasma.

In this Letter we apply the optical pump–THz probe spectroscopy to the study of multiphoton ionization of atmospheric gases. Our experimental scheme is outlined in Section 2. Section 3 describes a model of interaction of the THz radiation with photoionized gas plasma and presents a method of extraction of the plasma characteristics from experimental data. The experimental results presented in Section 4 are then interpreted in Section 5.

## 2. Experimental details

We employed an experimental setup typical for time-resolved THz studies [15] which is schematically shown in Fig. 1. As a laser source, we used a Quatronix Odin Ti:sapphire multipass femtosecond pulse amplifier. It generates 1 mJ laser pulses with a 55 fs temporal length, 810 nm mean wavelength and 1 kHz repetition rate. The output laser beam is divided into three parts. Up to 80% of the laser power is used to the ionization of the examined gas (oxygen or nitrogen) either directly or using the second harmonic generation (for 405 nm pump wavelength) in an LBO crystal. We used a setup which enables controlling the pump pulse polarization and fine tuning of its peak intensity [12]. About 20% of the laser power was used for the generation and gated detection of THz pulses. For this purpose we use a pair of 1 mm thick (1 1 0)-oriented ZnTe crystals [16]. The entire THz setup was enclosed in a box, which was evacuated, and then refilled with the examined gas at atmospheric pressure. The THz radiation was focused with a pair of ellipsoidal mirrors and a 0.5 mm aperture was placed into the common focal point of the optical pump and THz probe beams.

* Corresponding author. Fax: +420 286 890 527.
*E-mail address:* kuzelp@fzu.cz (P. Kužel).

0009-2614/$ - see front matter © 2008 Elsevier B.V. All rights reserved.
doi:10.1016/j.cplett.2008.09.046

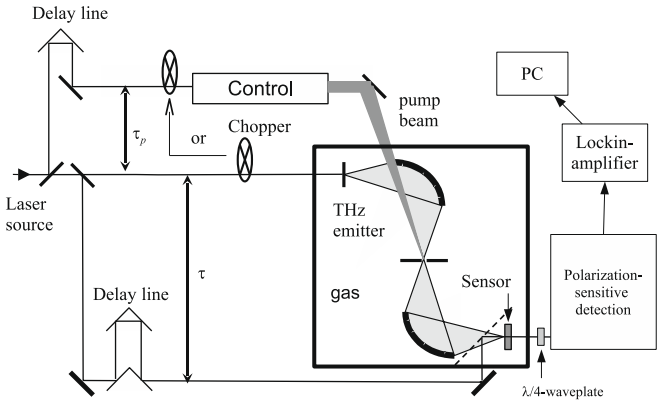


**Fig. 1.** Experimental scheme. The pump beam branch contains a specific arrangement for a careful control of the pump beam attenuation and polarization and a second harmonic stage. The chopper can be either in the probe branch measuring the THz field transmitted through the sample, or in the pump branch to measured the photoinduced change in the transmitted THz signal.

This alignment allowed us to quantify the volume and shape of the probed ionized gas column (see [12] for details). The problem of the effective interaction volume has been extensively discussed in the literature [17]. The pump beam intensity strongly varies within the space probed by THz radiation, which has a substantially broader waist than the focused optical pump. For high-order nonlinear processes far from saturation, which is our case, the transient signal comes essentially from the central part of the laser focus. Similarly as in Ref. [12] we consider the half width of the radial profile of the excitation density $I^n$ (where $n$ is the order of the nonlinearity) as a convenient approximation of the radius of the cylindrical interaction volume. It was shown that $n = 4$ constituted the right choice for $O_2$ pumped at 405 nm [12]: indeed, different values of $n$ yielded worse fits of the transient dielectric spectra and, finally, the free electron concentration deduced from the data was proportional to $I^4$. Similarly, we assumed the nonlinearity order of $n = 6$ in the estimation of the interaction volume for experiments with $N_2$. This choice was subsequently confirmed by the experimental results. Note that the dynamic range of our experiments with $N_2$ is then decreased compared to those with $O_2$ as the ratio between the THz beam cross-section and the cross-section of the interaction volume is increased for $N_2$ (i.e., less THz photons can interact with the plasma in the case of $N_2$ and the interaction should be stronger to yield the same signal level). The problem of determination of the interaction volume is also the main reason why we were not able to determine quantitatively the plasma characteristics for the excitation at 810 nm.

The time width of our THz pulses is ~1 ps. A non-collinear setup was used in our experiments with an angle of 10° between the pump and probe beams (Fig. 1). The non-collinearity of the pump and probe beams imply that the rise-time of the transient signal extends over a few ps; its decay then occurs at the time-scale of hundreds of ps. The pump–probe delay of 5–10 ps is then the earliest time, where the transient data can be quantitatively explored within the quasi-steady-state approximation (i.e., assuming the plasma does not change its state within the THz probe pulse length).

A synchronous detection scheme locked to a mechanical chopper operating at 166 Hz was used. Two delay lines controlled the time delay between the THz probe and optical sampling pulses (the sampling time $\tau$ makes connection to the real time of the experiment) and between the optical pump and THz probe pulses (pump-probe delay $\tau_p$). For the measured data we use the following notation. $E(\tau, \tau_p)$ is the THz wave form transmitted through the ionized gas at time $\tau_p$ after the photoionization event. $E(\tau)$ is the reference wave form, i.e., the THz wave form transmitted through the gas with pump beam off. $\Delta E(\tau, \tau_p) = E(\tau, \tau_p) - E(\tau)$ is the transient THz wave form; this quantity can be measured directly by placing the chopper into the pump branch. It reflects the changes in the gas induced by photoionization.

## 3. Interaction with probing radiation

The THz probing radiation strongly interacts with mobile delocalized carriers. Consequently, the coupling of the THz electric field to free electron plasma will dominate the interaction of the probing radiation with photo-ionized gas. This enables one to learn from transient THz dielectric spectra the free electron concentration and scattering rate at various levels of the pump intensity. In contrast, the ionized gas molecules are much heavier and their translational motion cannot be efficiently driven by the THz field.

To examine the dielectric response of the plasma, we measure the transient THz wave form $\Delta E(\tau, \tau_p)$ (i.e. $\tau$ is scanned while $\tau_p$ is set to 5–10 ps after photoionization). From that, the transient transmission function $\Delta t(\omega)$ of the plasma can be calculated using Fourier transformation:

$$\Delta t(\omega) = \Delta E(\omega; \tau_p)/E(\omega). \tag{1}$$

where $\Delta E(\omega; \tau_p)$ resp. $E(\omega)$ are $\Delta E(\tau; \tau_p)$ resp. $E(\tau)$ transformed into the frequency domain. It is then possible to evaluate the refractive index of the plasma from the equation (see Ref. [12] for a detailed description):

$$\Delta t(\omega) = \{\exp[\mathrm{i}\omega(n + \mathrm{i}\kappa)d_{\mathrm{eff}}/c] - 1\}\frac{V}{d_{\mathrm{eff}}S_{\mathrm{a}}}, \tag{2}$$

where $S_a$ is the opening of the aperture at the focus of the pump and THz beams, $d_{\mathrm{eff}}$ is the effective interaction length of the two beams (the effective length of the plasma column as 'seen' by the THz probing pulse), $V$ is the interaction volume (the volume of the probed part of the plasma cylinder). $\Delta N = n + \mathrm{i}\kappa$ is the pump-induced change in the refractive index. Eq. (2) assumes that the transmission losses due to inhomogeneities (i.e., partial reflections and scattering) can be neglected compared to those related to the propagation effects described by the exponential term. Finally, we get the complex permittivity of the plasma from the equation:

$$\varepsilon(\omega) = (1 + \Delta N)^2 \tag{3}$$

To fit these spectra, we use a Drude-Lorentz model [12]:

$$\varepsilon(\omega) = 1 - \frac{\omega_p^2}{\mathrm{i}\omega/\tau_s + \omega^2 - \omega_p^2/2} \tag{4}$$

where $\omega_p$ is the plasma frequency, which is connected with the free electron density $N_e$: $\omega_p^2 = N_e e^2/(\varepsilon_0 m_e)$. Here $e$ and $m_e$ are the electron charge and mass, respectively, and $\varepsilon_0$ stands for the vacuum permittivity. The term $\omega_p^2/2$ accounts for a restoring force which originates in a screening due to the spatial separation of positive ions and negative electrons [12]. This model allows us to determine the free electron density and their scattering rate for the experiments we carried out.

## 4. Experimental results

To examine the nature of the ionization processes we varied several parameters of the pump beam. We carried out the pump-probe experiments for two ionization wavelengths: 810 nm (the output wavelength of our laser source) and its second harmonics, i.e., 405 nm. Comparative measurements were performed with linearly and circularly polarized pump beams, where the polarization was modified using a $\lambda/4$-plate. Finally, we carefully varied the

intensity of the pump beam. The peak excitation intensity was calculated based on the measured pump power, the time length of the pulse and the size of the laser spot at the point of excitation. The spot size was measured by a CCD camera in the regime where the pump intensity was strongly attenuated. We estimate that the absolute value of the pump pulse peak intensity could be determined with an uncertainty factor better than 2 (i.e. twice smaller or twice larger than the calculated value). The random error within a series of measurements was much smaller and did not exceed 10%. The applied peak pump intensities are in the range 1–23 TW/cm$^2$ for 405 nm and 30–160 TW/cm$^2$ for 810 nm pump wavelengths.

In Fig. 2 we plot examples of transient dielectric spectra for the linearly polarized pump beam with a wavelength of 405 nm. We show here a comparison of the spectra obtained for the two gases at about the same pump intensity. During these measurements the pump-probe delay was fixed to a value such that the THz pulse probed the plasma ~5 ps after the photoionization. The signal oscillations for $N_2$ correspond to the noise level which is higher for experiments with nitrogen due to the decreased dynamic range as discussed in the experimental part.

We measured first the pump intensity dependence of the peak values of the THz transient wave forms (i.e. $\Delta E_{\max} = \Delta E(\tau, \tau_p)$, where $\tau$ was set to the maximum of the signal wave form). These measurements provide information only about the average THz response of the plasma. Nevertheless, they are fast and the temporal stability of the laser is sufficient to allow us to monitor precisely the highly nonlinear dependence of the signal versus the pump intensity. The values obtained during these measurements were then used to normalize the peaks of the entire transient THz wave forms which were measured subsequently. These latter measurements are slower but allow us to evaluate the plasma characteristics encoded into the THz signal transmitted through the photoexcited region.

The whole set of measurements allowed us to determine the electron density and scattering time versus the pump intensity [12]. The calculated electron densities obtained for pumping at 405 nm are displayed in Fig. 3. The scattering time of the free electrons was found to be (200 ± 50) fs for nitrogen (both for linear and circular polarizations) and (400 ± 50) fs for oxygen. In our earlier paper [12] we reported a small pump intensity dependence of the scattering time in oxygen (150–350 fs): this was caused by a numerical error in evaluation of our data which was fixed in the present Letter. Note that the values and variation of the electron plasma density presented and discussed in Ref. [12] are not influenced by this. The electron scattering time we find is clearly subpicosecond and it is independent of the pump intensity for both gases in our experimental conditions.

The 810 nm pump induces appreciable variation in the transmitted THz wave form only for intensities higher than about 30 TW/cm$^2$ as can be observed in the inset of Fig. 3. Qualitatively, the nonlinearity of these ionization processes is clearly higher than for 405 nm pump wavelength. However, for 810 nm excitation we were not able to evaluate quantitatively the plasma density. This is because the interaction volume $V$ for such highly nonlinear processes is rather small and is extremely difficult to evaluate; furthermore, approximations, under which Eq. (2) was derived, namely that of negligible Fresnel losses, is not fulfilled.

Finally, we carried out comparative measurements of the peaks of the THz signal wave form for linear ($\Delta E_{\text{lin}}$) and circular ($\Delta E_{\text{circ}}$) polarization of the pump beam. We measured both $\Delta E_{\text{lin}}$ and $\Delta E_{\text{circ}}$ with variable pump intensity at wavelengths of 405 and 810 nm. The ratio of the measured values $\Delta E_{\text{circ}}/\Delta E_{\text{lin}}$ for oxygen and 405 nm pump beam is 0.7 at 4 TW/cm$^2$ and slowly decreases

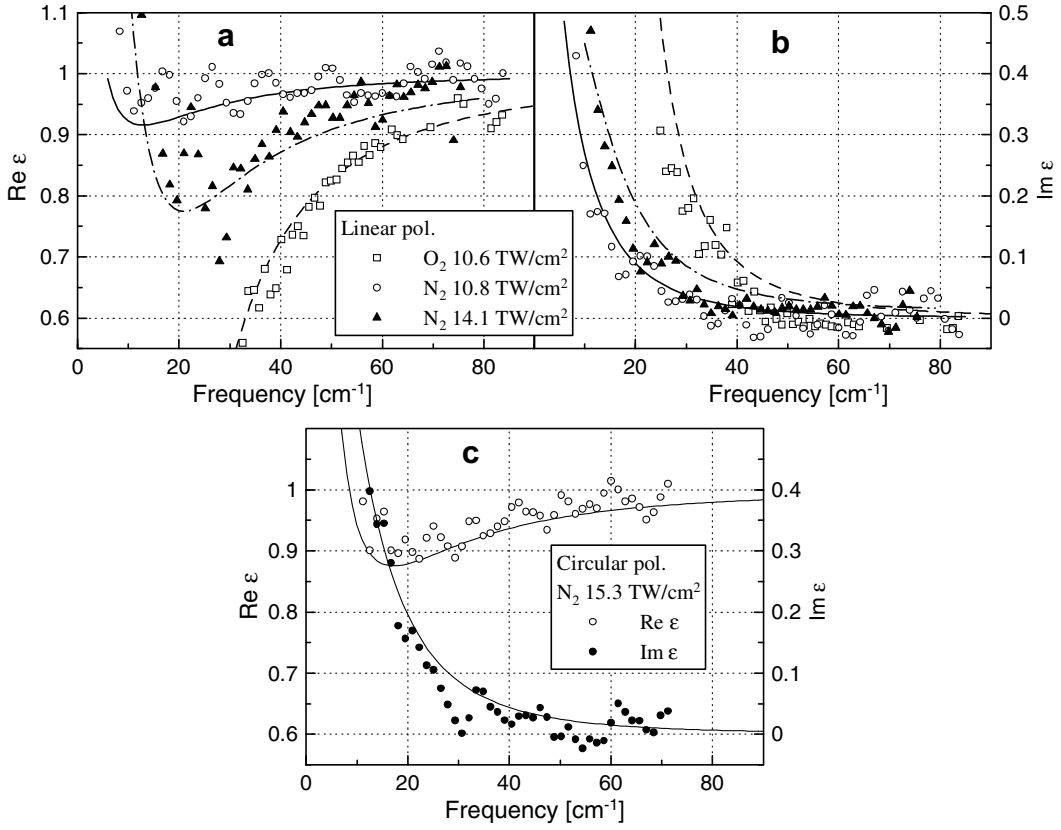


**Fig. 2.** Examples of dielectric spectra of photoionized oxygen and nitrogen; pump at 405 nm; panels (a) and (b): linear polarization; panel (c): circular polarization. Symbols: experimental data; lines: fit by Eq. (4).

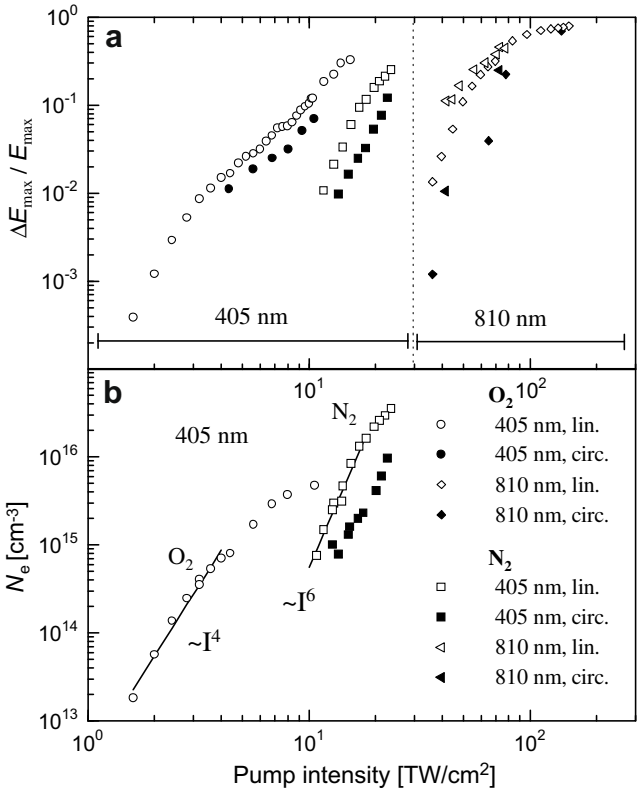


**Fig. 3.** (a) Peak transient THz signal versus the pump intensity for excitation wavelengths 405 and 810 nm for linear and circular polarization (raw data). (b) Density of free electrons versus the pump intensity for 405 nm pump wavelength and linear polarization. The low-intensity part of these dependences can be fitted by simple power laws $\propto I^4$ for $O_2$ and $\propto I^6$ for $N_2$ indicating 4-photon and 6-photon processes.

to about 0.6 at 12 TW/cm$^2$. For nitrogen these values are found in the range of ~0.4–0.5 at 405 nm (Fig. 3a). The comparison of the density of free electrons obtained from the fits of dielectric spectra for linear and circular polarization in nitrogen reveals similar differences. In contrast, at 810 nm the ionization rate with the circularly polarized beam is at relatively small pump intensities (where the probing signal does not reach saturated regime) for both gases strongly reduced compared to the experiments with linearly polarized beam; $\Delta E_{circ}/\Delta E_{lin} \approx 0.1$.

## 5. Discussion

The adiabatic ionization potential for oxygen is $E_B = 12.07$ eV. For the 405 nm excitation wavelength (photon energy of 3.06 eV), at least four photons are required to ionize the $O_2$ molecule.

The ionization process can be described by the strong-field approximation proposed by Reiss [18] which consists in neglecting of the influence of the binding potential on the detached electron in comparison with the oscillating high-frequency laser field effects. In this state the electron acquires a 'quiver' or ponderomotive energy given by [3]:

$$U_P = e^2 E_L^2/(4m_e\omega_L^2), \tag{5}$$

where $E_L$ is the intensity and $\omega_L$ the frequency of the laser field. It is generally accepted that multiphoton ionization channels may open and close at some specific values of the pump intensity $I_L \propto E_L^2$ [3]. This is related to the fact that the electrons, when ejected into a strong laser field, need to overcome the sum of the ionization and ponderomotive potentials. Following Eq. (5) this value increases with increasing laser intensity. Consequently, the $n$-photon ionization channel closes when $U_P$ reaches such value that [19]:

$$n\hbar\omega_L = E_B + U_P. \tag{6}$$

It means that at lower laser intensities than those required to fulfill the condition (6) the $n$-photon process represents the lowest order ionization path. In the dipole approximation the relevant transition matrix element is approximately proportional to $\propto \langle \Psi_f | r^n | \Psi_i \rangle$ [20], where $\Psi_i$ is the initial (bound) state wave function and $\Psi_f$ is the final (delocalized) state one. This term usually dominates in the multiphoton ionization process. At higher intensities, the energy of $n$ photons becomes too low and an additional photon is required to ionize the molecule; $(n+1)$-photon process becomes dominant [19]. In our case Eqs. (5) and (6) yield a value of $I_L \approx 11$ TW/cm$^2$ for closing the 4-photon channel. This seems to be in a good agreement with the saturation of the free electron density progressively as this irradiance value is approached (Fig. 3). Similar levelling-off of the signal at pump intensities below the channel-closing threshold were observed in recent optical pump-probe experiments in isooctane [19].

The ionization potential of nitrogen is 15.60 eV [21]. It means that $5 \times 3.06 = 15.3$ eV is slightly below the threshold. It follows, in agreement with our experimental results that the 6-photon ionization process largely dominates over the whole range of pump pulse intensities. The 6-photon channel closing would occur at about 180 TW/cm$^2$ and no conclusive levelling-off of the signal thus could be observed in our experiments. We observe in Fig. 3 that an efficient generation of electrons starts now at higher pump intensities than for $O_2$ due to the higher order process involved.

The polarization of the ionizing radiation can have a dramatic effect on the nature of the ionization process. As has been shown in [20], excitation with a circularly polarized beam drives the detached electrons into free states $\Psi_f(l)$ with a high angular momentum quantum number $l$ creating thus a centrifugal barrier for ionization. The measure of the barrier is the overlap between the functions $r^n\Psi_i$ and $\Psi_f(l)$. It has been shown by photoelectron spectroscopy in xenon gas [20] that in this situation the near threshold ionization transitions can be inhibited and higher-order processes turn on and appear as higher energy peaks in the photoelectron spectrum.

We think that the situation is quite analogous in our experiments, however our experiments do not give direct access to the photoelectron energy. For 405 nm pump with linear polarization the $n$th order process (where $n = 4$ for $O_2$ and $n = 6$ for $N_2$) dominates while a significant contribution of the $(n+1)$th order process may come into play for the experiments with the circular polarization. The role of this process [i.e. the respective weight of populations of electrons created by $n$- and $(n+1)$-photon processes] then should depend on how large the excess energy of free electrons is with respect to the single photon energy $\hbar\omega_L$. Concerning the ionization of $N_2$ with circularly polarized light at 405 nm, we dispose of data in a relatively narrow pump intensity range. Nevertheless, within the experimental accuracy, the average slope of the electron density versus intensity is close to 6 similarly as in the case of the linear pump polarization. We believe that this means qualitatively that the centrifugal barrier does not surmount the high excess energy for the 6-photon process, i.e. in the mixture of 6- and 7-photon processes the lower order process dominates. Even higher order processes involved in the experiments with 810 nm pump imply a higher centrifugal barrier and lower photon excess energy; consequently, a larger difference between the experiments with circular and linear polarizations is observed.

The scattering time of the free electrons was found to be independent of the pump intensity at 405 nm. It is 200 fs for nitrogen and 400 fs for oxygen. These numbers are compatible with those obtained for $O_2$ by Kampfrath and al. [14]. However, in that paper

the authors worked with significantly higher plasma densities where the scattering of electrons on oxygen ions plays an important role. In our experiments the scattering of free electrons on neutral molecules dominates. As the scattering cross section of the free electrons is about the same in oxygen and nitrogen ($\sigma \sim 10^{-19}$ m$^2$ [22,23]), the lower electron scattering time in nitrogen can be explained only by the higher velocity of the generated free electrons. Indeed, for the 6-photon process in nitrogen, the energy of the photons exceeds the ionization threshold by 2.8 eV, whereas for oxygen the sum of energy of the four photons is almost equal to the ionization potential of an $O_2$ molecule. The excess energy of 2.8 eV corresponds to the electron velocity of $v = 1 \times 10^6$ m/s. Taking into account that the momentum scattering time $\tau$ of free electrons is equal to

$$\tau = \frac{1}{\sigma N_0 v}, \tag{7}$$

where $N_0 = 2.7 \times 10^{19}$ cm$^{-3}$ is the concentration of gas molecules at atmospheric pressure, the value of the electron scattering time in nitrogen can be estimated: $\tau \approx 350$ fs. This is in a good semi-quantitative agreement with the experiment (given the uncertainty in the value $\sigma$ for example).

In this approximation, the twice higher scattering time observed for oxygen implies a four times lower excess energy of electrons (0.7 eV). This value overestimates the excess energy for the four photon ionization process in $O_2$. Or, in other words, given the theoretical value of free electron excess energy, a surprisingly low scattering time (high collision rate) was observed. High electron collision rates in oxygen have been also found previously in similar experimental conditions [14]. In that paper multi-THz pulses were used to probe the electron plasma at higher densities (i.e., $N_e > 10^{17}$ cm$^{-3}$). In this regime the electron scattering on ions dominates. Progressively, as the electron density is decreased down to $N_e \sim 10^{15}$–$10^{16}$ cm$^{-3}$, which corresponds to our experimental conditions, the scattering on ions vanishes and collisions with neutral molecules prevail. The collision rate of $1/\tau = 2.5$ THz deduced from our experiments matches well the extrapolation of the data shown in [14] towards low $N_e$ confirming the unexpectedly low electron scattering time in $O_2$.

## 6. Summary

We have applied optical pump–THz probe spectroscopy to examine laser-induced ionization in oxygen and nitrogen at atmospheric pressure. Free electron densities in the range $10^{13}$–$10^{17}$ cm$^{-3}$ were inferred from the THz data for the pump pulse peak intensities in the range 1–23 TW/cm$^2$ at 405 nm. The dielectric properties of the generated plasma were determined and interpreted in the framework of the multiphoton ionization process.

## Acknowledgements

The support by the Ministry of Education and the Grant Agency of the Czech Republic (projects LC512 and 202/06/0286) is gratefully acknowledged. One of the authors (S.E.B.) is supported by the National Science Foundation (Grant No. CHE-0617060).

## References

[1] N.B. Delone, V.P. Krainov, Multiphoton Processes in Atoms, Springer, Heidelberg, 2000.
[2] S.M. Hankin, D.M. Villeneuve, P.B. Corkum, D.M. Rayner, Phys. Rev. A 64 (2001) 013405.
[3] M. Protopapas, C.H. Keitel, P.L. Knight, Rep. Prog. Phys. 60 (1997) 389.
[4] C. Ellert, P.B. Corkum, Phys. Rev. A 59 (1999) R3170.
[5] I.V. Litvinyuk, K.F. Lee, P.W. Dooley, D.M. Rayner, D.M. Villeneuve, P.B. Corkum, Phys. Rev. Lett. 90 (2003) 233003.
[6] R.J. Levis, M.J. Dewitt, J. Phys. Chem. A 103 (1999) 6493.
[7] S. Champeaux, L. Berge, Phys. Rev. E 71 (2005) 046604.
[8] A. Petrignani, W.J.V.D. Zande, P.C. Cosby, F. Hellberg, R.D. Thomas, M. Larsson, J. Chem. Phys. 122 (2005) 014302.
[9] E.C. Zipf, J. Geophys. Res. 85 (1980) 4232.
[10] B.D. Sharpee, T.G. Slanger, D.L. Huestis, P.C. Cosby, Astrophys. J. 606 (2004) 605.
[11] S.P. Jamison, J. Shen, D.R. Jones, R.C. Issac, B. Ersfeld, D. Clark, D.A. Jaroszynski, J. Appl. Phys. 93 (2003) 4334.
[12] Z. Mics, F. Kadlec, P. Kužel, P. Jungwirth, S.E. Bradforth, V.A. Apkarian, J. Chem. Phys. 123 (2005) 104310.
[13] T. Kampfrath, L. Perfetti, D.O. Gericke, C. Frischkorn, P. Tegeder, M. Wolf, Chem. Phys. Lett. 429 (2006) 350.
[14] T. Kampfrath, D.O. Gericke, L. Perfetti, P. Tegeder, M. Wolf, C. Frischkorn, Phys. Rev. E 76 (2007) 066401.
[15] H. Němec, F. Kadlec, S. Surendran, P. Kužel, P. Jungwirth, J.Chem.Phys. 122 (2005) 104504.
[16] A. Nahata, A.S. Weling, T.F. Heinz, Appl. Phys. Lett. 69 (1996) 2321.
[17] J.H. Posthumus, Rep. Prog. Phys. 67 (2004) 623.
[18] H.R. Reiss, Phys. Rev. A 22 (1980) 1786.
[19] A.T. Healy, S. Lipsky, D.A. Blank, J. Chem. Phys. 127 (2007) 214508.
[20] P.H. Bucksbaum, M. Bashkansky, R.R. Freeman, T.J. Mcilrath, Phys. Rev. Lett. 56 (1986) 2590.
[21] G. Herzberg, Molecular Spectra and Molecular Structure, Van Nostrand Rheinhold, New York, 1950.
[22] K.P. Subramanian, V. Kumar, J. Phys. B: At. Mol. Opt. Phys. 23 (1990) 745.
[23] Y. Itikawa et al., J. Phys. Chem. Ref. Data 15 (1986) 985.